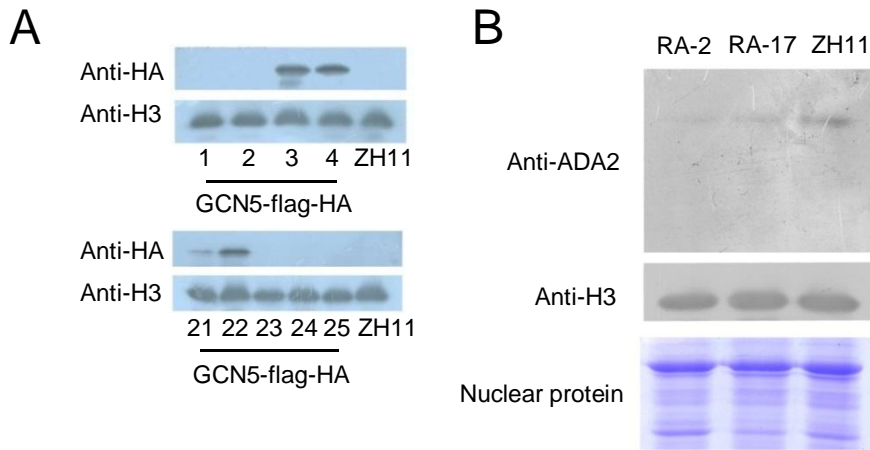
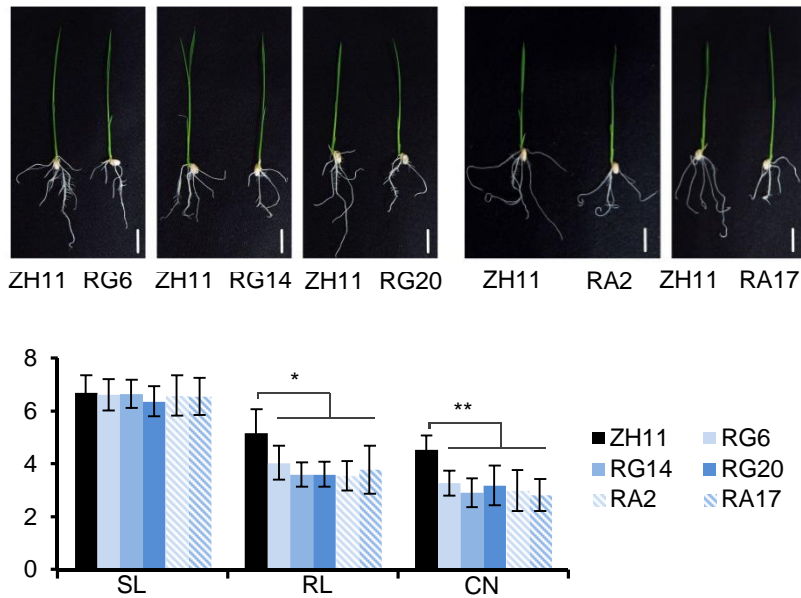


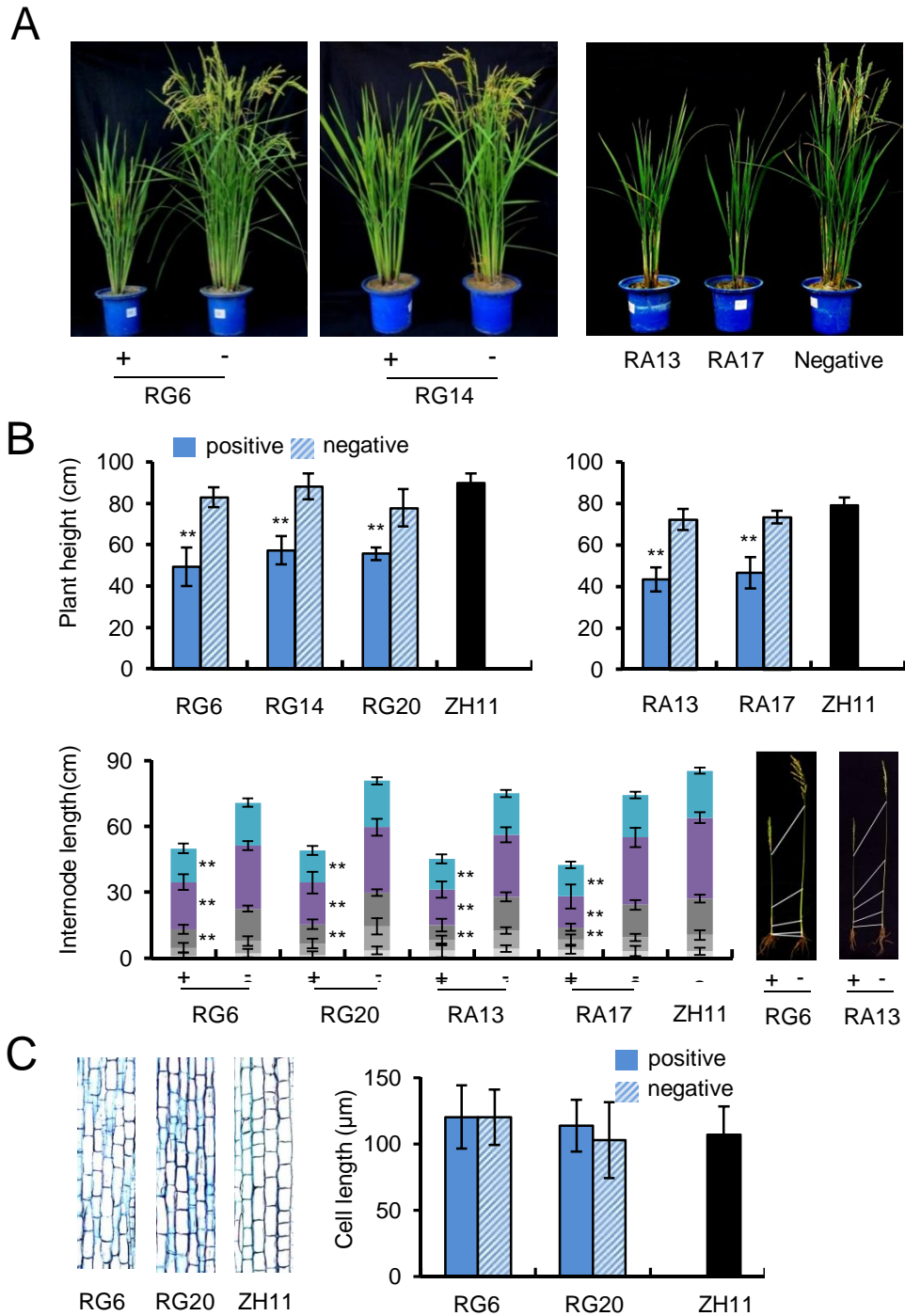
Supplemental Figure 1 (Supports Figure 1). Mapping the interaction regions of ADA2, GCN5, and WOX11 by yeast two-hybrid assays and comparison of their expression profiles in rice tissues/organs. (A) Schematics of *WOX11*, *ADA2*, and *GCN5* structures and truncated segments used for interaction assays. **(B)** Interaction of AD (the prey plasmid pGADT7) fusions of truncated ADA2 with BD (the bait plasmid pGBKT7) fusions of truncated WOX11 or full-length GCN5. Yeast cells transformed with different combinations of plasmids were grown on the SD-LT and SD-LTHA media. X-gal assays were performed. **(C)** Detection of *GCN5*, *ADA2*, and *WOX11* transcripts by RT-qPCR in roots (R⁰), intercalary meristem of young stem (St), 5 day seedling (Se), 5cm panicle (Pa), and mature leaf (Le). Bars are means \pm SD from three technical replicates.



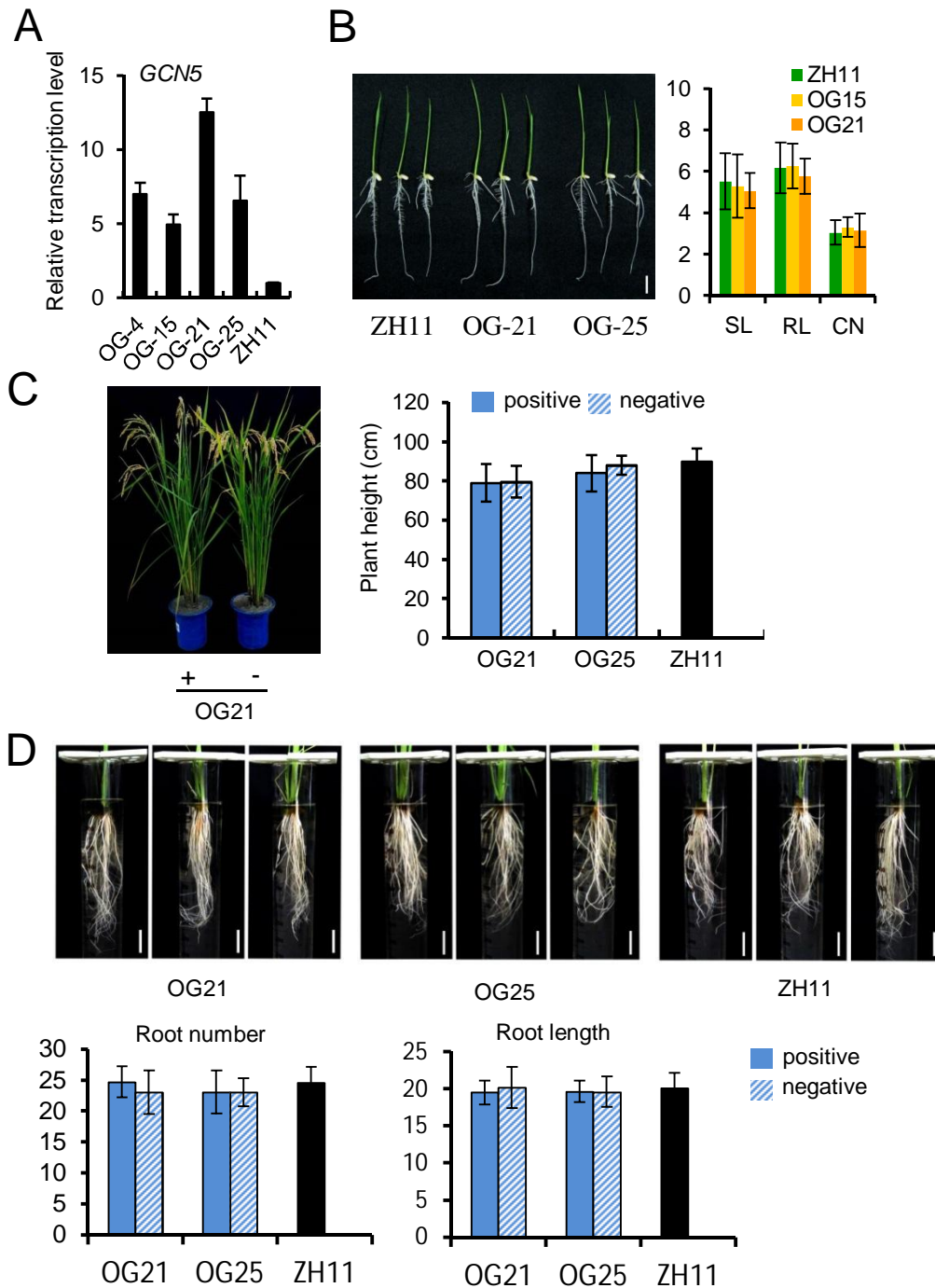
Supplemental Figure 2 (Supports Figure 1 and Figure 3). Protein levels of GCN5 and ADA2 in transgenic plants. (A). Detection of GCN5-HA fusion protein levels in 9 transgenic lines and wild type (ZH11) by immunoblots with anti-HA antibody. Anti-H3 was used as a control. **(B).** Detection of ADA2 protein levels in two *ADA2* RNAi lines and wild type (ZH11) by immunoblots using polyclonal anti-ADA2 antibody. Anti-H3 was used as a control.



Supplemental Figure 3 (Supports Figure 3). Root phenotypes of *GCN5* and *ADA2* RNAi seedlings with the same shoot length as wild type. Upper, phenotype of *GCN5* and *ADA2* RNAi and wild type (ZH11) with the same shoot length. *GCN5* and *ADA2* RNAi seeds were germinated 1.5 days before ZH11 to obtain the same shoot length. bars=1cm. Lower, Statistical data from the *GCN5* and 2 *ADA2* RNAi lines. SL, shoot length. RL, root length. CN, crown root number. Bars are means \pm SD of 10 plants. Significant difference between transgenic lines and wild type (Student's *t* tests, P value<0.05 or 0.01) are marked by single or double asterisks.

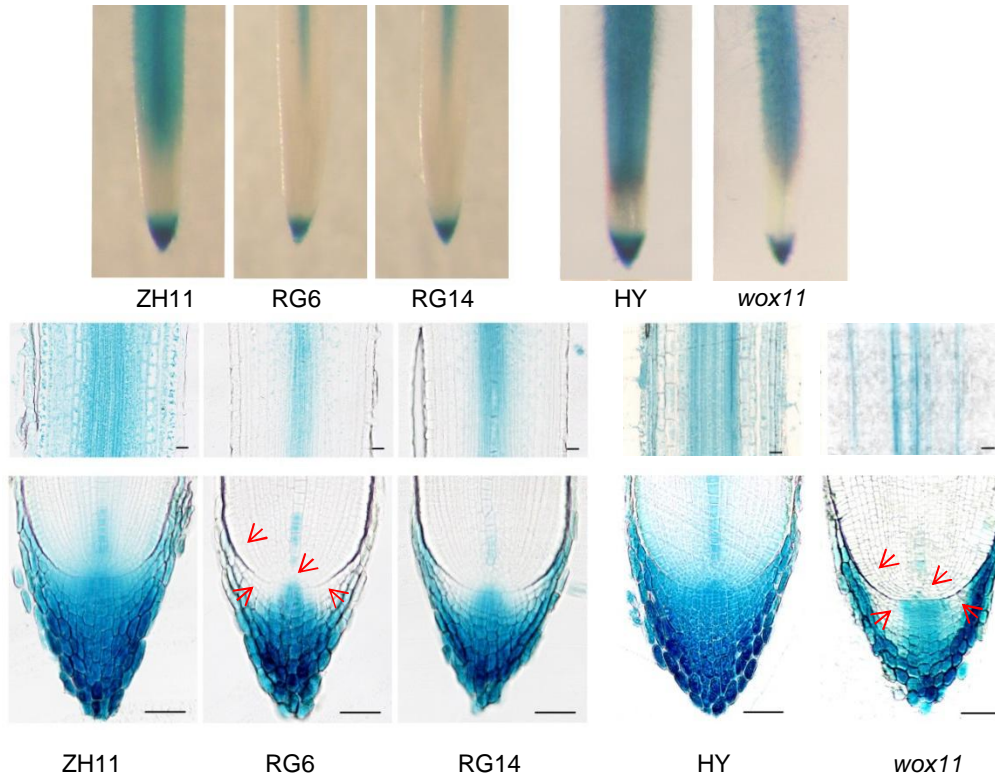


Supplemental Figure 4 (Supports Figure 3). Phenotypes of *GCN5* and *ADA2* RNAi lines at mature stages. (A) Phenotype of positive (+) and negative (-) (without the transgene) segregates of *GCN5* RNAi and over-expression lines. **(B)** Statistical data of plant height and/or internode length of *GCN5* RNAi and *ADA2* RNAi lines. Error bars= means \pm SD. Significant difference (Student *t*'s test, P value<0.01) between positive plants and negative plants or wild type were marked by two asterisks. **(C)** Comparison of epidermal cell length between *GCN5* RNAi line and wild type (ZH11).

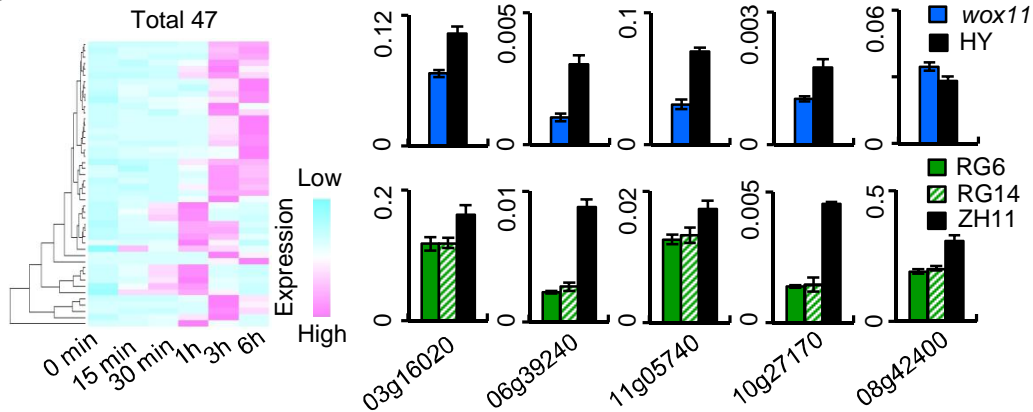


Supplemental Figure 5 (Supports Figure 3). Production and phenotype of *GCN5* overexpression lines. (A) RT-qPCR analysis of *GCN5* transcripts in 4 transgenic lines and wild type (ZH11). Values are relative to *ACTIN1* transcripts. Bars are means \pm SD from three technical replications. **(B and C)** No obvious phenotype observed in *GCN5* over-expression lines compared with wild type. **(B)** seedlings at day 7 after germination. **(C)** OG21 positive and negative segregants at mature stage. Statistical data from 2 over-expression lines (OG-21 and OG-25) and wild type are shown. Bars represent means \pm SD. **(C)** Comparison of root number and length of 45-day-old hydroponic *GCN5* over-expression and wild type plants. Scale bars = 3cm. Statistical data from positive and negative segregants of OG-21 and OG-25 lines and wild type are shown in the lower panel.

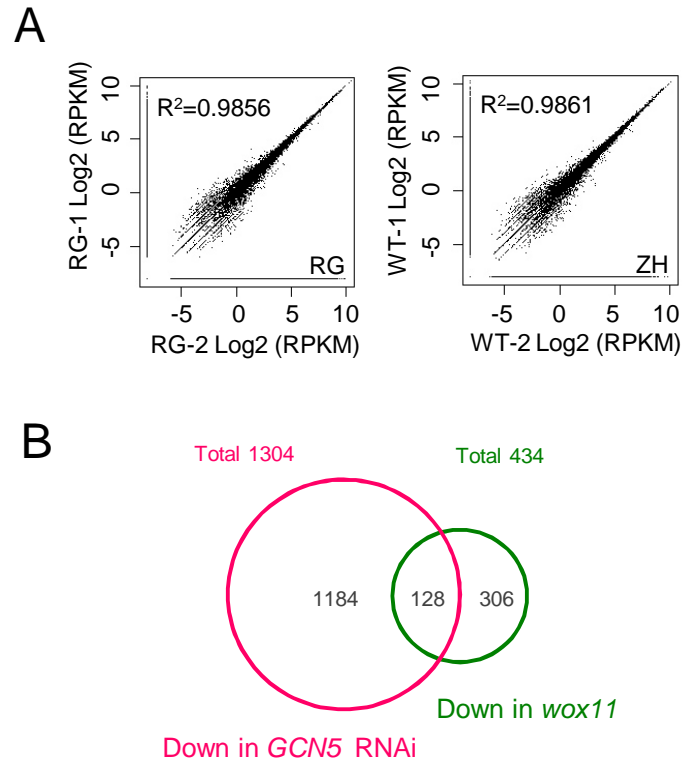
A



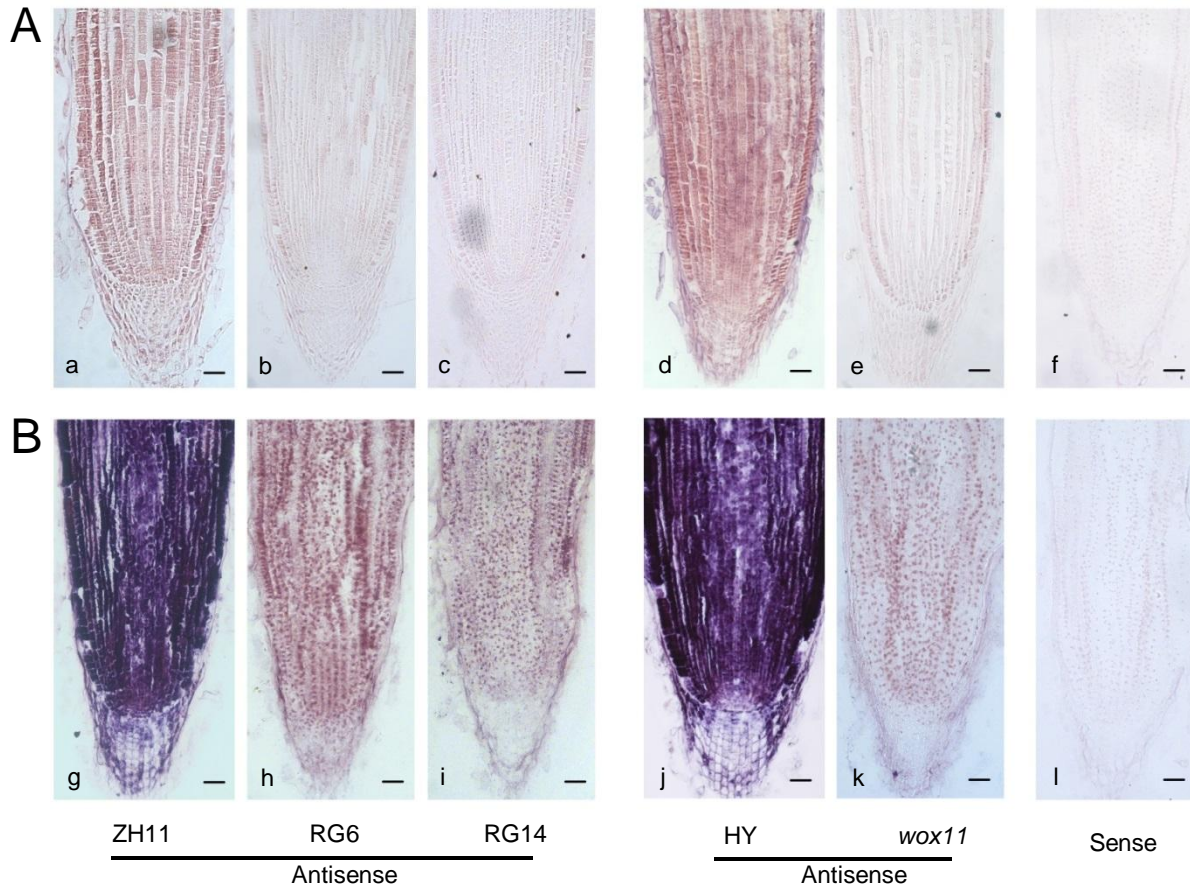
B



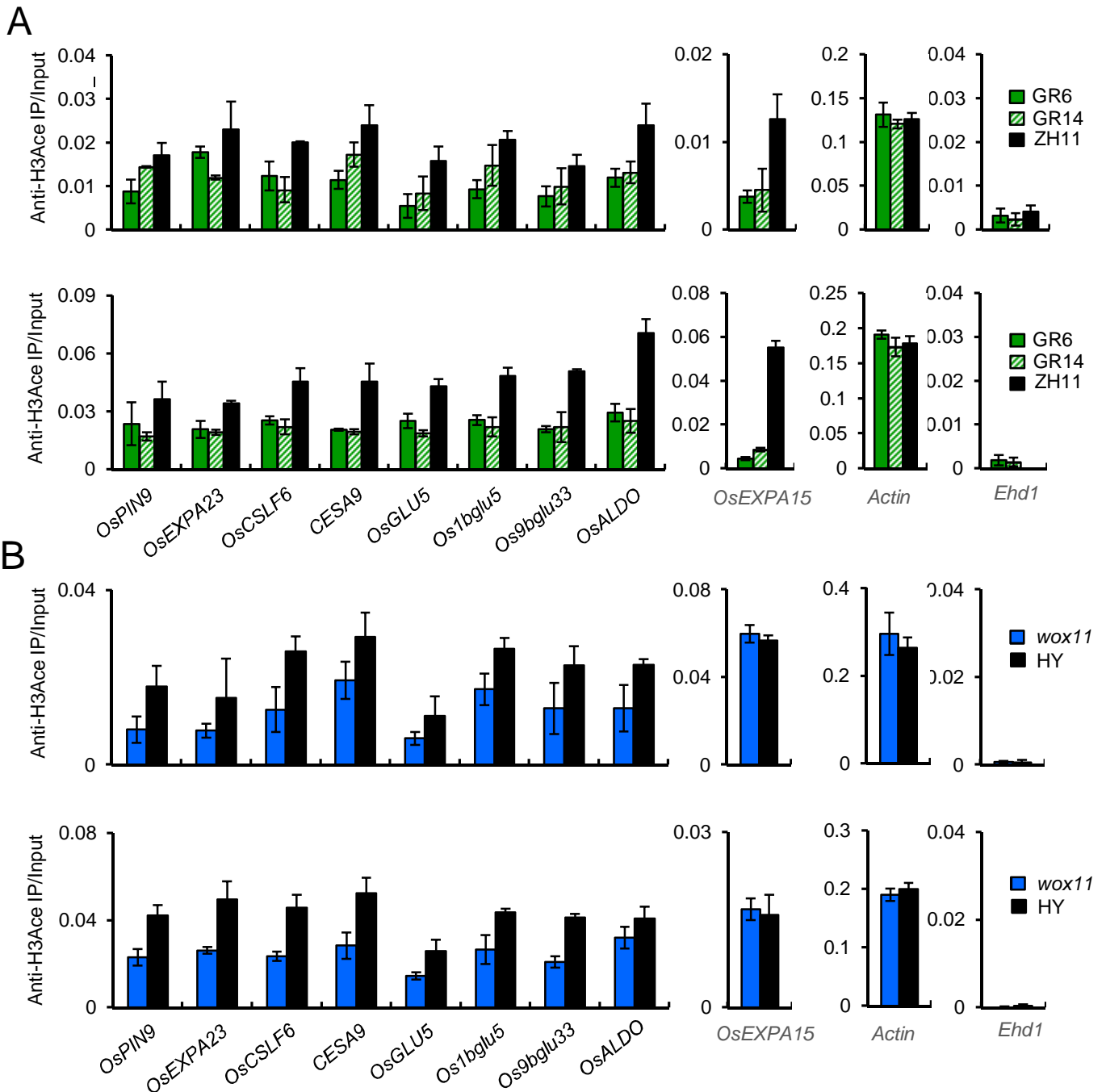
Supplemental Figure 6 (Supports Figures 4 to 7). *GCN5* and *WOX11* are required for auxin accumulation or response in crown root tip. (A) Upper panels, examination of *DR5:GUS* expression by GUS staining in roots of *GCN5* RNAi lines, *wox11* mutant, and the corresponding wild type, ZH11 and HY, respectively. Middle and lower panels, enlarged views of longitudinal sections of root differentiation zones and meristem zones. Red arrows indicates the regions with much lower *DR5:GUS* expression in *GCN5* RNAi lines or *wox11* mutant compared with wild type. Bars = 50 μ m. **(B)** Left, heat map of transcripts induced by auxin of *GCN5* regulated auxin inducible genes. Right, several auxin inducible genes are down-regulated in *GCN5* RNAi and *wox11* mutant. 08g42400 is used as a negative control, which is down-regulated in *GCN5* RNAi but not in *wox11* mutant.



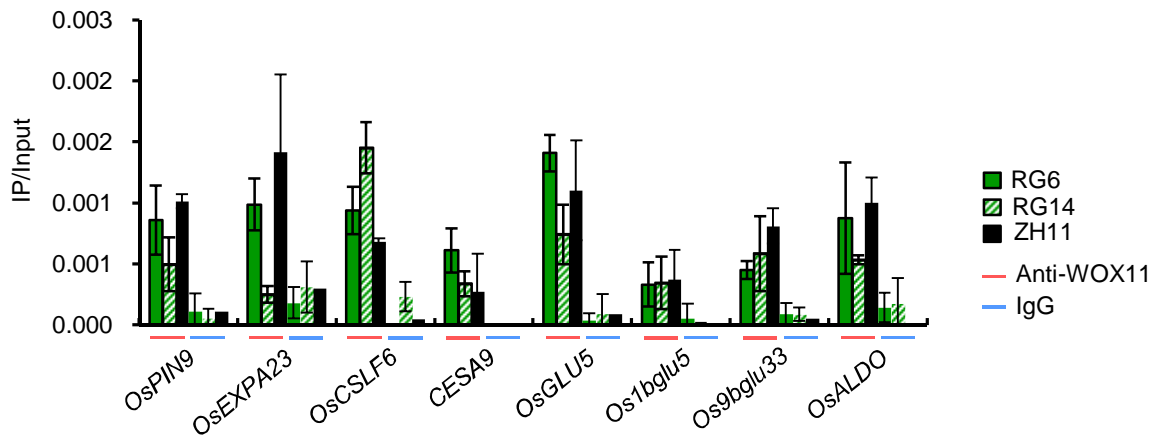
Supplemental Figure 7 (Supports Figure 5). RNA-seq analysis of *GCN5* RNAi plants and comparison with down-regulated genes in *wox11* root tips. (A) Correlation of the crown root tip RNA-seq replicates by two-wise scatter plot. **(B)** Overlapping of down-regulated genes in crown root tips of *GCN5* RNAi and *wox11* mutant seedlings.



Supplemental Figure 8 (Supports Figure 6). *In situ* hybridization detection of *OsPIN9* and *OsCSLF6* transcripts in crown root tip of two *GCN5* RNAi lines, *wox11* mutant, and their corresponding wild types. (a to e, g to k), antisense probe. (f, l), sense probe control. Bars = 25 μ m.



Supplemental Figure 9 (Supports Figure 7). The other two biological replicates of the H3 acetylation ChIP-qPCR assays shown in Fig 7A, B. Left histograms are ChIP assays with anti-H3Ace of 8 common target genes in roots of two *GCN5* RNAi lines compared with wild type (ZH11) (A), and *wox11* mutant compared with wild type (HY) (B). Histograms in the right side are tests of *OsEXPA15* and *Actin* loci as controls. Bars represent means \pm SD from three technical repeats. For the biological replicates in A and B, crown roots from 2 independent germinations for each genotype were used for the ChIP analysis.



Supplemental Figure 10 (Supports Figure 7). GCN5 RNAi does not affect WOX11 binding to target genes. ChIP assays were performed using anti-WOX11 antibody with roots of wild type and two GCN5 RNAi lines. Anti-IgG was used as controls.

Supplemental Table 1: RNA-seq reads and analysis data.

Line		Raw reads	Clean reads	Mapped reads	Unmapped reads
RG-1	Left reads	35323265	35310748 (99.96%)	30915215 (87.56%)	4392600 (12.44%)
	Right reads	35323265	35269495 (99.85%)	30213452 (86.78%)	4603244 (13.22%)
RG-2	Left reads	35574250	35565540 (99.98%)	31254470 (87.89%)	4308372 (12.11%)
	Right reads	35574250	35522748 (99.86%)	30608454 (87.24%)	4478009 (12.76%)
WT-1	Left reads	27670810	27662015 (99.97%)	24547199 (88.75%)	3112758 (11.25%)
	Right reads	27670810	27622220 (99.82%)	23896903 (87.85%)	3303807 (12.15%)
WT-2	Left reads	32621071	32589206 (99.90%)	28878952 (88.62%)	3707804 (11.38%)
	Right reads	32621071	32550549 (99.78%)	28293208 (87.98%)	3867198 (12.02%)

Supplemental Table 2. Gene ontology analysis of down-regulated genes by *GCN5* RNAi.

GO ID	GO Name	RG down	All gene	P value
GO:0005975	carbohydrate metabolic process	48	600	0
GO:0006073	cellular glucan metabolic process	8	30	0
GO:0006333	chromatin assembly or disassembly	1	928	0
GO:0006468	protein amino acid phosphorylation	31	1593	0
GO:0006508	proteolysis	36	3377	0
GO:0006629	lipid metabolic process	36	280	0
GO:0006808	regulation of nitrogen utilization	10	30	0
GO:0006869	lipid transport	19	106	0
GO:0006979	response to oxidative stress	29	186	0
GO:0007047	cellular cell wall organization	23	132	0
GO:0008152	metabolic process	166	1968	0
GO:0009664	plant-type cell wall organization	12	42	0
GO:0009765	photosynthesis, light harvesting	16	17	0
GO:0015979	photosynthesis	31	177	0
GO:0016068	type I hypersensitivity	25	283	0
GO:0044237	cellular metabolic process	17	133	0
GO:0046274	lignin catabolic process	7	26	0
GO:0055114	oxidation reduction	107	1199	0
GO:0007155	cell adhesion	3	418	0.0001
GO:0015995	chlorophyll biosynthetic process	6	21	0.0001
GO:0042309	homiothermy	90	1647	0.0001
GO:0050826	response to freezing	90	1647	0.0001
GO:0006950	response to stress	19	204	0.0002
GO:0006952	defense response	9	626	0.0003
GO:0016042	lipid catabolic process	8	48	0.0003
GO:0006915	apoptosis	7	532	0.0004
GO:0009853	photorespiration	3	5	0.0005
GO:0019253	reductive pentose-phosphate cycle	3	5	0.0005
GO:0046677	response to antibiotic	7	48	0.0016
GO:0006006	glucose metabolic process	4	15	0.0018
GO:0006886	intracellular protein transport	1	214	0.0023
GO:0019953	sexual reproduction	6	39	0.0026
GO:0009239	enterobactin biosynthetic process	9	84	0.0031
GO:0015904	tetracycline transport	6	41	0.0033
GO:0015031	protein transport	2	245	0.0037
GO:0006633	fatty acid biosynthetic process	12	139	0.004
GO:0006826	iron ion transport	5	30	0.0041
GO:0030418	nicotianamine biosynthetic process	2	3	0.0041
GO:0006412	translation	20	863	0.0049

GO:0030001	metal ion transport	11	129	0.0061
GO:0030245	cellulose catabolic process	4	21	0.0062
GO:0030244	cellulose biosynthetic process	5	34	0.0069
GO:0009058	biosynthetic process	17	251	0.0076
GO:0009813	flavonoid biosynthetic process	2	4	0.0079
GO:0006457	protein folding	17	254	0.0083
